THE INFLUENCE OF GROUND CONTROL POINTS IN THE TRIANGULATION OF LEICA ADS40 DATA

S. Alhamlan [a] *, J. P. Mills [a], A. S. Walker [b], T. Saks [c]

[a] School of Civil Engineering and Geosciences, University of Newcastle, UK – (s.m.alhamlan, j.p.mills)@ncl.ac.uk
[b] Leica Geosystems GIS and Mapping, LLC, USA – stewart.walker@gis.leica-geosystems.com
[c] Leica Geosystems GIS and Mapping GmbH, Switzerland – tauno.saks@gis.leica-geosystems.com

Commission I, WG I/6

KEY WORDS: Accuracy, ADS40, Aerial Triangulation, Bundle Adjustment, Digital Sensor, Precision

ABSTRACT:

This paper is concerned with the influence of ground control points (GCPs) on the aerial triangulation of datasets acquired using a Leica ADS40. The ADS40 comprises seven parallel linear sensors in the focal plane of a single lens system. Three panchromatic sensors scan the same ground area at different angles to acquire forward, nadir and backward scenes. After the raw imagery and metadata are downloaded, determination of exterior orientation parameters and subsequent image rectification enable stereo viewing in three possible geometric combinations. Residual parallax in the rectified data, however, means bundle adjustment is necessary before the maximum photogrammetric accuracy can be achieved. In order to assess the influence of bundle adjustment, a dataset of ADS40 imagery was acquired for an 8 x 8 km study area around Waldkirch in Switzerland. The dataset consists of four adjacent strips of ADS40 imagery plus two cross strips scanned by each of the sensor's seven channels. The ADS40 imagery of the study area was pre-processed, rectified and triangulated interactively using the ADS40 ground processing software GPro, the SOCET SET® photogrammetric software suite and the ORIMA bundle adjustment software. Repeated triangulation of the dataset in different configurations of strips, scenes and GCPs was applied. The number of GCPs was increased gradually in different arrangements to assess the influences on the triangulation process and analyse the need for GCPs when using GPS/IMU data. Based on the findings, recommendations are made as to the most suitable block configuration to be selected when using data of this kind.

1. INTRODUCTION

This paper reports on the influence of ground control points (GCPs) in the aerial triangulation of datasets acquired using Leica Geosystems' Airborne Digital Sensor, the ADS40. The Leica ADS40 comprises seven parallel linear sensors (three panchromatic and four multispectral channels), placed next to one another in the focal plane of a single lens system. The panchromatic sensors scan the same ground area at different angles to acquire forward, nadir and backward scenes (Figure 1).

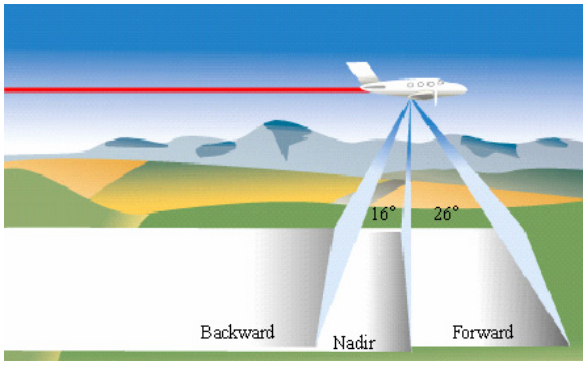

Figure 1. Forward (F), Nadir (N) and Backward (B) scenes (image courtesy Leica Geosystems GIS and Mapping)

After the raw imagery and metadata are downloaded, the determination of exterior orientation parameters (based on position and attitude data from the integrated GPS/IMU system) and subsequent image rectification is possible. Consequently, stereo viewing in three combinations of two panchromatic bands, i.e. forward/nadir (F/N), forward/backward (F/B) and nadir/backward (N/B) is enabled. Nevertheless, at this stage the rectified data is insufficient for photogrammetric measurement because of the remaining parallax in the rectified images (present, for example, as result of any misalignment between the IMU and camera axes and the datum between GPS/IMU and the ground control system), necessitating photogrammetric bundle adjustment.

In order to assess the influence of bundle adjustment on imagery of this type, a dataset of ADS40 imagery was acquired for an 8 x 8 km study area around Waldkirch in Switzerland. The dataset consists of four adjacent strips of ADS40 imagery plus two cross strips scanned by each of the sensor's seven channels. The ADS40 imagery of the study area was pre-processed, rectified and triangulated interactively using the ADS40 ground processing software GPro, the BAE Systems SOCET SET® photogrammetric software suite and the Leica ORIMA bundle adjustment software. Repeated triangulation of the dataset in different configurations of strips, scenes and GCPs was applied. The number of GCPs was increased in different arrangements to assess the influences of the triangulation process and analyse the need for the GCPs in the presence of GPS/IMU data. To achieve this, three phases of testing were designed, with measurements taking place as follows:-

Phase I: Block I (four parallel strips), pre-triangulation.
Phase II: Block I, post-triangulation.

* Corresponding author.

Phase III: Block II (two additional cross strips), post-triangulation.

This paper summarises the outcomes of the testing. Based on the findings of the research, recommendations are made as to the most suitable block configuration to be selected when using ADS40 data of this kind.

2. TEST DATA AND SOFTWARE

2.1 Test data

The dataset made available for the study consisted of six strips of ADS40 imagery with the characteristics shown in Table 1.

ADS40 imagery	Six strips with GPS/IMU data
Coverage	8 x 8 km
Location	Waldkirch, Switzerland
No. of GCPs	30
Focal length	62.5 mm
Flying height	2000 m
Pixel size	6.5µm
GSD	200 mm

Table 1. Test data characteristics

2.2 Software

Software made available for the purpose of conducting the study comprised:

- ADS40 ground processing software, GPro (v. 2.18)
- SOCET SET photogrammetric software suite (v. 4.3.1)
- ORIMA bundle adjustment software (v. 6.0)

3. PHASE I: BLOCK I, PRE-TRIANGULATION

3.1 GPS/IMU Processing and image rectification

The raw ADS40 images were first resampled to remove the influences of the aircraft movement during image acquisition. This was performed using position and attitude data from a variant of the Applanix Position and Orientation System (POS) developed to meet the requirements of the ADS40 sensor (Sandau et al., 2000). Data was collected synchronously with image acquisition and processed relative to a GPS base station. This stage of the pre-processing was performed in-house by Leica Geosystems, investigation of this aspect of the processing flowline being beyond the scope of this research study. Rectification of the ADS40 imagery was performed, in order to produce stereo-viewable images, using GPro. The first stage of the study was concerned with assessing the three possibilities for stereo viewing of the rectified panchromatic images, i.e. F/N, F/B and N/B scene configurations, as described by Templemann et al. (2000).

3.2 Assessment of different stereo configurations

The three different stereoscopic combinations were assessed using stereo measurements of 18 independent GPS coordinated check points. Figure 2 shows the check points that were available for measurement using the SOCET SET photogrammetric software suite.

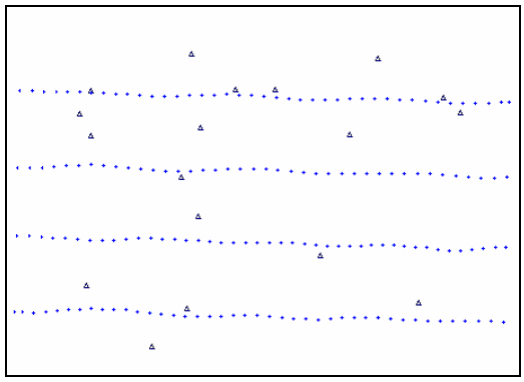

Figure 2. Location of the independent check points available for stereo measurement

The final results of stereo measurements for each combination are presented in Table 2. Each different measurement combination produced different results, partly as a consequence of the different stereo angles (Figure 1). A reasonable RMS of approximately two pixels was present in the horizontal components (X, Y), however the vertical component (Z) was greater than six pixels in each combination, which does not satisfy the requirements of photogrammetric measurement. The three different possible stereo configurations were therefore considered in the subsequent phases of this study to find the impact of each combination on photogrammetric application.

Scene combination	RMS X (m)	RMS Y (m)	RMS Z (m)
F/N	0.323	0.267	1.316
F/B	0.358	0.247	1.263
N/B	0.431	0.204	1.310

Table 2. RMS of Phase I stereo measurements

4. PHASE II: BLOCK I, POST-TRIANGULATION

4.1 Block I triangulation

The quality of the georectified imagery may be improved through triangulation in order to achieve a higher level of precision and accuracy. The four parallel strips of rectified imagery were therefore triangulated using ORIMA; first of all without and subsequently with three different configurations of GCPs. Four different combinations (F/N, F/B, N/B and F/N/B) of the three panchromatic scenes were triangulated.

4.2 Ground control point configurations

The GCPs configurations, selected as subsets from the dataset of 30 GPS coordinated ground points provided, comprised zero, four, nine and 12 GCPs (Appendix A, Figures A1 to A4).

4.3 Results from Block I adjustments

The Combined Adjustment Program for Aerial Triangulation (CAP-A), which is fully integrated into the working environment of ORIMA, was used to perform a bundle adjustment for the 16 block combinations. Accordingly CAP-A outputs were checked to eliminate blunders. Errors affecting σ_0 and each ORIMA block output were analysed. The final adjustment precisions for each triangulation are listed in Table 3.

Scene combination	Block I (four strips) σ_0 (μm)			
	0 GCPs	4 GCPs	9 GCPs	12 GCPs
F/N	3.2	3.4	3.3	3.4
F/B	4.1	4.1	4.3	4.2
N/B	2.8	2.8	2.9	2.9
F/N/B	3.4	3.4	3.4	3.4

Table 3. Phase II ORIMA σ_0 results

It is noted that importing GCPs in different patterns had only a slight effect on the adjustment precision of the two scene block combinations. Triangulating three panchromatic scenes produced a weighted average of the two scene adjustments.

4.4 Stereo measurement tests

The independent check points described in Figure 2 were measured in SOCET SET. Stereo measurements were made to 24 combinations of ADS40 images (the F/N/B triangulation has three stereo possibilities, namely F/N, F/B and N/B). A summary of the results from the stereo measurements is given in Appendix B. The importing of GCPs into the triangulation process resulted in an improvement in the accuracy of measurement. The check points in the F/N/B triangulation were measured in the three stereo combinations to determine which stereo possibility should be used to achieve the optimal result. It is clear that triangulated combinations without GCPs returned the lowest accuracy, particularly in the vertical component. The importing of four GCPs into the bundle adjustment improved the accuracy significantly in all combinations. The influence of importing one, two and three GCPs to the triangulation process is therefore now being investigated to see if this eliminates what is believed to be a "datum" problem with the vertical component. Increasing the GCP count to nine improved the measurement accuracy further. In the case of the 12 GCP configurations, no improvement was made to the measurement accuracy, indeed a slight degradation was evident from the graphs. This is suspected to be as a result of an erroneous GCP, but further investigations are ongoing.

It can be summarised that for optimum results, all three panchromatic scenes should be used in the triangulation process. The F/B stereo combination produced the optimum stereo measurements and the use of nine GCPs in the block provided the best solution for this phase of testing.

5. PHASE III: BLOCK II, POST-TRIANGULATION

5.1 Block II triangulation

In Phase III, the two cross strips were added to the adjustment so that six strips were used in the triangulation. The procedures followed in phase II were repeated in order to study the impact of importing cross strips into the triangulation together with different GCP patterns. The same panchromatic scene combinations as described in Section 4.1 were adopted.

5.2 Ground Control point configurations

The GCPs configurations, selected as subsets from the provided dataset, comprised zero, four, nine and 12 GCPs and were located as shown Appendix A (Figures A5 to A8).

5.3 Results from Block II adjustments

Each ORIMA output was analysed after running CAP-A and areas of weakness identified to fulfil the required criteria. The final results (σ_0) of CAP-A adjustments are listed in Table 4.

Scene combination	Block II (six strips) σ_0 (μm)			
	0 GCPs	4 GCPs	9 GCPs	12 GCPs
F/N	3.8	3.6	3.6	3.6
F/B	4.5	4.3	4.3	4.3
N/B	3.3	3.2	3.2	3.2
F/N/B	3.8	3.8	3.8	3.8

Table 4. Phase III ORIMA σ_0 results

It is noted that adding cross strips produced a slightly degraded precision in comparison with Phase II (Table 3). Importing GCPs in different patterns again had minimal effect on the adjustment precision of different scene combinations.

5.4 Stereo measurement tests

The stereo observation process used in phase II was repeated for the Block II (six strips) adjustments. The same independent check points were used in the stereo measurement test. Appendix C summarises the results of the 24 sets of measurements. In this case it is noted that adding cross strips without GCPs did not significantly improve the vertical stereo measurements accuracies. Therefore, importing GCPs is still required to maximise the height accuracy.

6. CONCLUDING REMARKS

The results presented in this paper show that, despite the presence of GPS/IMU data, the digital aerial triangulation of ADS40 images still requires some GCPs in order to maximise photogrammetric precision and accuracy. All three panchromatic scenes (F, N and B) should be used in triangulation to achieve optimum results. For optimum stereo plotting results, the F/B panchromatic scenes (comprising the largest stereo angle of all scene combinations) should be adopted. Finally, the addition of cross strips minimizes the number of GCPs required to four in the corners of the block. Adopting these guidelines resulted in a near-homogeneous stereo measurement accuracy of 1 pixel in X, Y and Z axes (with measurements undertaken by a relatively inexperienced photogrammetric operator in the form of a research student).

REFERENCES

Sandau, R., Braunecker, B., Driescher, H., Eckardt, A., Hilbert, S., Hutton, J., Kirchhofer, W., Lithopoulos, E., Reulke, R. and Wicki, S., 2000. Design Principles of the LH Systems ADS40 Airborne Digital Sensor. *International Archives of Photogrammetry and Remote Sensing*, Amsterdam, The Netherlands, Vol. XXXIII, Part B2, pp. 258-265.

Tempelmann, U., Börner, A., Chaplin, B., Hinsken, L., Mykhalevych, B., Miller, S., Recke, U., Reulke, R. and Uebbing, R., 2000. Photogrammetric software for the LH Systems ADS40 Airborne Digital Sensor. *International Archives of Photogrammetry and Remote Sensing*, Amsterdam, The Netherlands, Vol. XXXIII, Part B2, pp. 552-559.

APPENDIX A

A.1 Block I (four strip) configurations

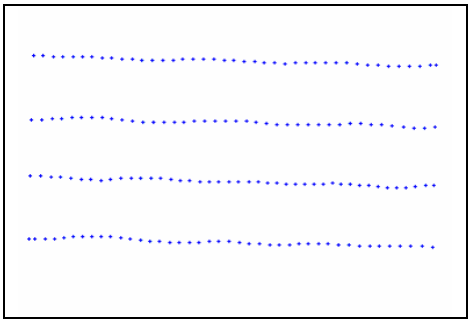

Figure A1. Four strips without GCPs

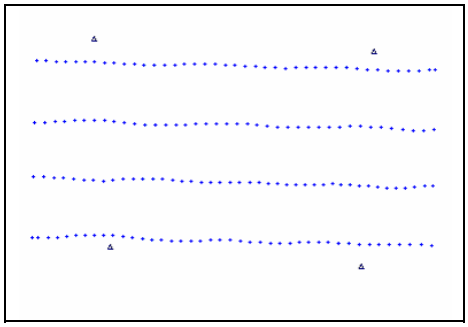

Figure A2. Four strips with 4 GCPs

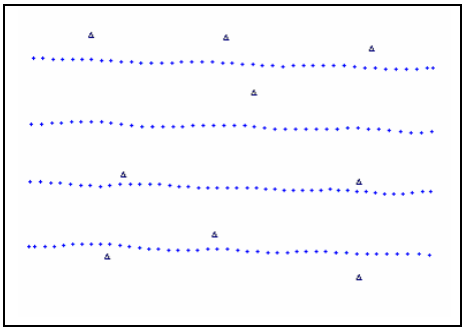

Figure A3. Four strips with 9 GCPs

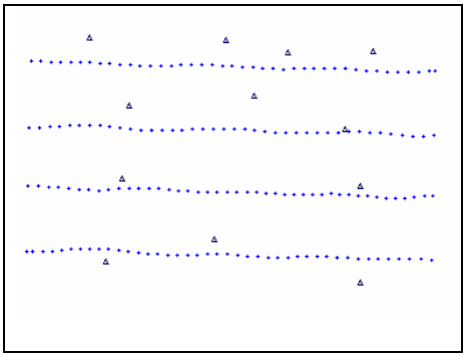

Figure A4. Four strips with 12 GCPs

A.2 Block II (six strip) configurations

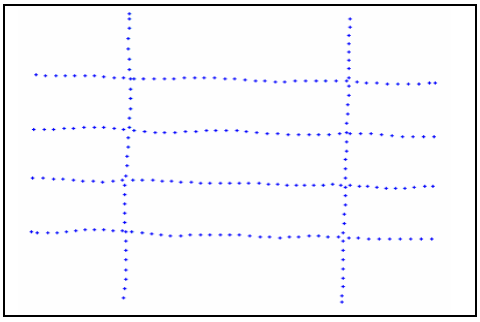

Figure A5. Six strips without GCPs

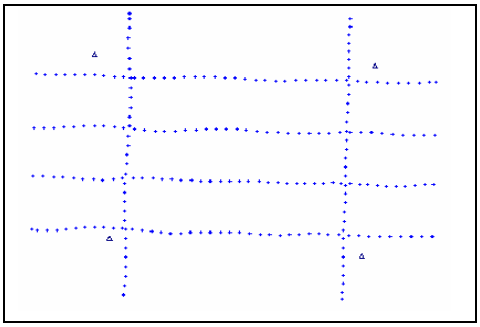

Figure A6. Six strips with 4 GCPs

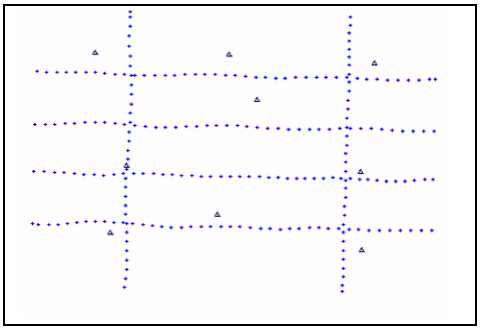

Figure A7. Six strips with 9 GCPs

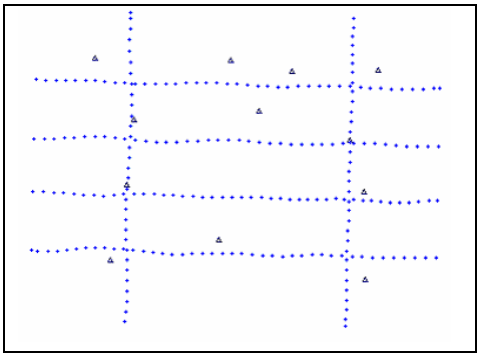

Figure A8. Six strips with 12 GCPs

APPENDIX B

Block I (four strips) RMS results for stereo measurements

Config.	GCPs	RMS X (m)	RMS Y (m)	RMS Z (m)
1	0	0.342	0.229	1.039
2	4	0.172	0.212	0.342
3	9	0.160	0.154	0.252
4	12	0.275	0.245	0.337

Table B1. RMS of F/B scene combination

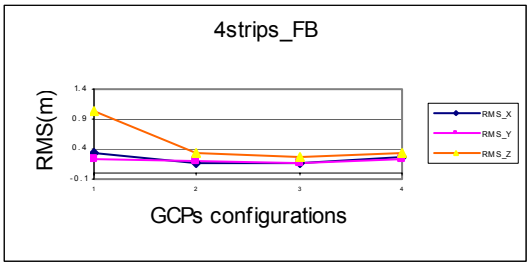

Figure B1. RMS of F/B scene combination

Config.	GCPs	RMS X (m)	RMS Y (m)	RMS Z (m)
1	0	0.359	0.215	0.875
2	4	0.144	0.164	0.440
3	9	0.191	0.161	0.324
4	12	0.291	0.224	0.333

Table B2. RMS of F/N scene combination

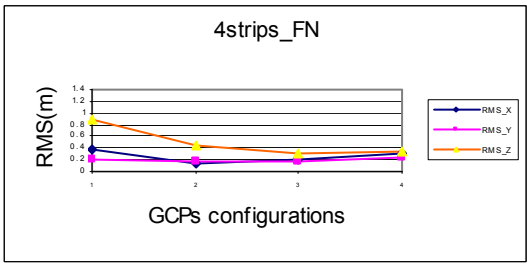

Figure B2. RMS of F/N scene combination

Config.	GCPs	RMS X (m)	RMS Y (m)	RMS Z (m)
1	0	0.384	0.263	1.042
2	4	0.176	0.242	0.584
3	9	0.158	0.246	0.471
4	12	0.278	0.264	0.623

Table B3. RMS of N/B scene combination

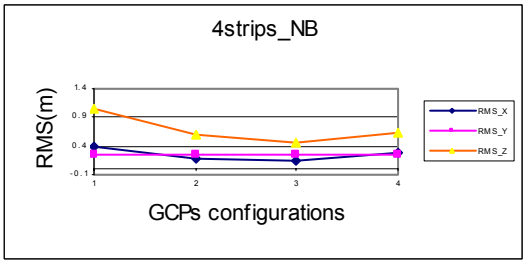

Figure B3. RMS of N/B scene combination

Config.	GCPs	RMS X (m)	RMS Y (m)	RMS Z (m)
1	0	0.308	0.242	1.165
2	4	0.178	0.230	0.401
3	9	0.212	0.201	0.236
4	12	0.272	0.210	0.266

Table B4. RMS of F/B scenes from F/N/B combination.

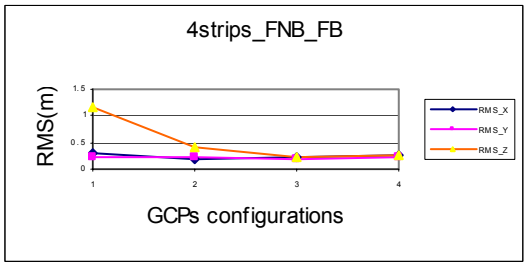

Figure B4. RMS of F/B scenes from F/N/B combination

Config.	GCPs	RMS X (m)	RMS Y (m)	RMS Z (m)
1	0	0.286	0.208	1.178
2	4	0.202	0.243	0.515
3	9	0.234	0.200	0.222
4	12	0.200	0.189	0.261

Table B5. RMS of F/N scenes from F/N/B combination

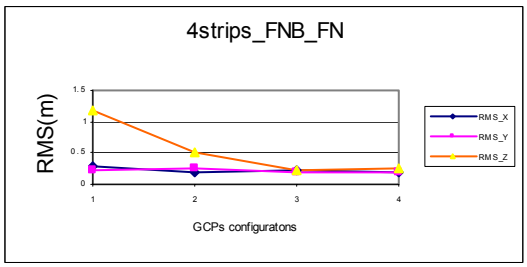

Figure B5. RMS of F/N scenes from F/N/B combination

Config.	GCPs	RMS X (m)	RMS Y (m)	RMS Z (m)
1	0	0.284	0.245	1.267
2	4	0.164	0.225	0.608
3	9	0.159	0.198	0.458
4	12	0.269	0.197	0.505

Table B6. RMS of N/B scenes from F/N/B combination

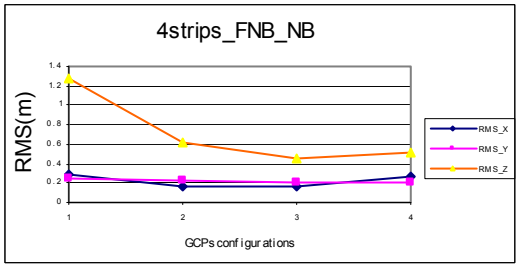

Figure B6. RMS of N/B scenes from F/N/B combination

APPENDIX C

Block II (six strips) RMS results for stereo measurements

Config.	GCPs	RMS X (m)	RMS Y (m)	RMS Z (m)
1	0	0.328	0.183	1.252
2	4	0.241	0.213	0.208
3	9	0.230	0.178	0.262
4	12	0.287	0.239	0.192

Table C1. RMS of F/B scene combination

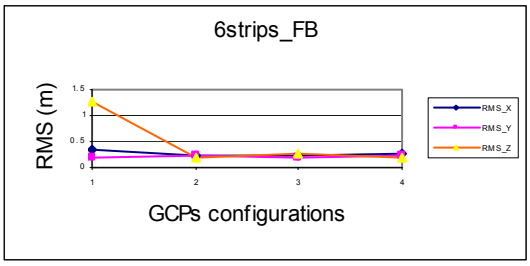

Figure C1. RMS of F/B scene combination

Config.	GCPs	RMS X (m)	RMS Y (m)	RMS Z (m)
1	0	0.335	0.178	1.187
2	4	0.167	0.165	0.371
3	9	0.188	0.123	0.294
4	12	0.261	0.177	0.304

Table C2. RMS of F/N scene combination

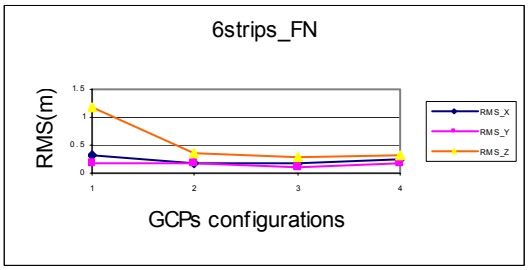

Figure C2. RMS of F/N scene combination

Config.	GCPs	RMS X (m)	RMS Y (m)	RMS Z (m)
1	0	0.312	0.201	1.354
2	4	0.200	0.195	0.603
3	9	0.183	0.212	0.593
4	12	0.238	0.246	0.651

Table C3. RMS of N/B scene combination

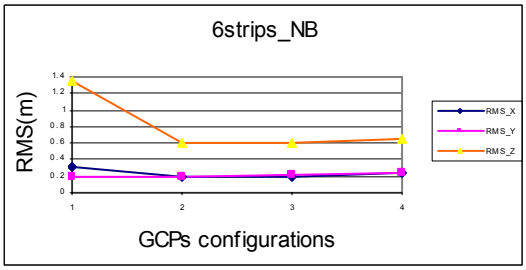

Figure C3. RMS of N/B scene combination

Config.	GCPs	RMS X (m)	RMS Y (m)	RMS Z (m)
1	0	0.325	0.214	1.247
2	4	0.247	0.177	0.247
3	9	0.198	0.146	0.176
4	12	0.279	0.217	0.236

Table C4. RMS of F/B scenes from F/N/B combination

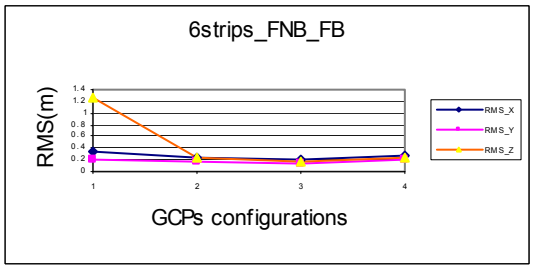

Figure C4. RMS of F/B scenes from F/N/B combination

Config.	GCPs	RMS X (m)	RMS Y (m)	RMS Z (m)
1	0	0.296	0.159	0.975
2	4	0.174	0.174	0.304
3	9	0.169	0.156	0.272
4	12	0.214	0.182	0.266

Table C5. RMS of F/N scenes from F/N/B combination

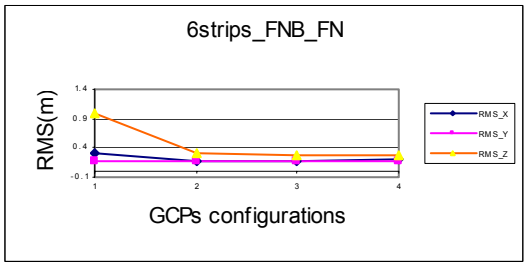

Figure C5. RMS of F/N scenes from F/N/B combination

Config.	GCPs	RMS X (m)	RMS Y (m)	RMS Z (m)
1	0	0.353	0.220	1.033
2	4	0.187	0.246	0.550
3	9	0.188	0.160	0.493
4	12	0.240	0.193	0.623

Table C6. RMS of N/B scenes from F/N/B combination

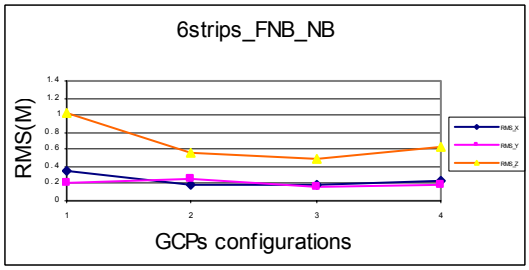

Figure C6. RMS of N/B scenes from F/N/B combination